Multipolar SPM machines for direct drive application: a comprehensive design approach

Multipolar SPM machines for direct drive application: a comprehensive design approach

B. Boazzo, G. Pellegrino, A. Vagati
Politecnico di Torino
Corso Duca degli Abruzzi 24, Torino, 10129 Italy

***Abstract* -- A closed-form, per-unit formulation is proposed, for the design of surface mounted permanent magnet motors with high number of poles. The model evaluates the shear stress, the power factor and the specific Joule loss as the indicators of the machine performance, and demonstrates that this is determined by the correct choice of a very limited set of key-geometrical parameters. The design criteria are described analytically and then applied to example designs, FEA validated. Distributed- and concentrated-winding configurations are considered. The conclusions of the paper are consistent with the literature and aim to give a roadmap for designers of PM machines in modern applications, such as wind power synchronous generators.**

Index Terms – PM motor drives, PM machines, Wind generation, Motor Design, Surface Mounted PM machines.

I. INTRODUCTION

Permanent magnet (PM) synchronous machines are recognized for their performance in terms of torque density, efficiency and low rotor inertia. In particular, direct-drive machines of the surface mounted PM type (SPM) have been increasingly adopted as motor and/or generators in many up to date fields such as traction and propulsion, aerospace and renewable energy production [1]. Recently, rare earth PM materials have suffered a significant volatility, but still the interest for PM based electrical machines is high, as stated in recent works [2].

All direct-drive machines have in common the high number of poles. Over the last decade, a lot of effort has been devoted to the investigation of machines with concentrated stator windings, for their characteristics of fault tolerance, ease of manufacturing, short end connections and high copper filling factor [2-7].

The paper proposes a normalized analysis of three-phase SPM machines, for the sake of sizing and preliminary design of direct-drive motor/generators. The analysis is based on simple, per-unit, relationships, including distributed and concentrated, single layer, winding types.

The proposed model is based on the elementary block reported in Fig. 1, representing one pole of a SPM machine with distributed windings. The key-geometric parameters, defined in Fig. 1, are:

- the airgap length g;
- the pole pitch a;
- the tooth length l_t;
- the PM length l_m.

For concentrated windings, the same geometric parameters are used, being a still the rotor pole pitch, corresponding to one PM pole. Another key parameter is the number of slot per pole per phase q, that can be either an integer or a fraction.

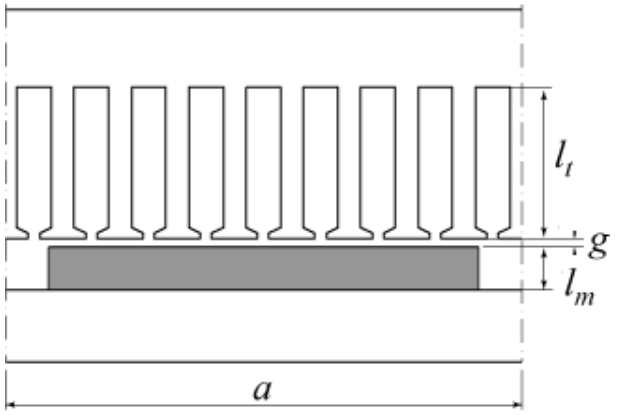

Figure 1. Elementary block of a linear-like SPM synchronous machine, corresponding to one PM pole pitch.

In the following, the relationships between the geometry, the shear stress (easily related to torque density), the power factor (PF) and the Joule loss per surface will be expressed by means of simple equations. It will be demonstrated that optimal combinations of the geometric quantities can maximize the power factor at a specified shear stress and vice versa. The emphasis on the power factor (read inner power factor or cosine of the torque angle) as a key design target has a twofold, strong motivation:

- the power factor determines the power converter current size, given the machine active power [8];
- a low power factor in a SPM machine is also the symptom of an armature flux that is not negligible with respect to the PM flux linkage one and that can require the magnetic core size to be augmented purposely.

II. PER UNIT MACHINE MODEL

A. Magnetic loading and rotor parameters

The magnetic loading (1) is defined as the peak of the fundamental component of the flux density distribution at the airgap at no load:

$$B = \hat{B}_{gap,fund} = k_b \cdot \frac{B_r}{1 + k_c \cdot \frac{g}{l_m}} \qquad (1)$$

Where B_r is the PM remanence, k_b is the PM shape coefficient relating the PM pitch to the fundamental flux density component at the airgap and k_c is the Carter coefficient. Apart from the Carter coefficient, the magnetic loading depends on rotor parameters only, given the airgap length, and it is ***independent of the rotor pole pitch a***.

The PM thickness factor l_m/g determines the magnetic loading (1) and also the de-magnetization current limit of the machine. High values such as $l_m/g > 6$ do not increase B significantly, and can be justified only if high current overload is required or anyway for avoiding de-magnetization. The example value $l_m/g = 6$ will be considered in the following and final designs will be verified against de-magnetization.

B. Electric loading and shear stress

The electric loading is defined in (2):

$$A = \frac{3}{2} \cdot \frac{N}{a} \cdot k_w \cdot I_q \qquad (2)$$

k_w in (2) is the winding factor, N is the number of conductors in series per pole per phase and I_q is the phase current amplitude. It is implicitly intended that the current vector is aligned with the quadrature axis, that is the maximum force (torque) per Ampere situation.

The average shear stress is:

$$\sigma = BA \qquad (3)$$

The shear stress is measured in N/m^2 and is the time-averaged tangential force acting on the elementary block of Fig. 1 divided by the airgap surface. In case of a cylindrical machine, the shear-stress is representative of its torque capability.

Once the magnetic loading is set, according to the PM grade, shape and thickness (1), the shear stress will depend on the electric loading (2) only. This can be upper limited either by Joule losses (i.e. thermal issues and efficiency) or by de-magnetization. Plus, the power factor can also set a limitation to the feasible electric loading, in particular in fractional slot machines.

Joule loss

The Joule loss factor k_j represents the copper loss per airgap unit surface, expressed in W/m^2:

$$k_j = \frac{2\rho_{Cu} k_{end}}{k_{Cu}(1 - k_t \cdot B/B_{fe})} \left(\frac{A}{k_w}\right)^2 \frac{1}{l_t} \qquad (4)$$

ρ_{Cu} in (4) is the copper resistance, k_{Cu} is the slot filling factor, k_{end} is the length of the conductors including the end connections divided by their active length. B_{fe} is the peak flux density in the stator yoke, and k_t is the tooth scaling factor, accounting for the tooth width and, consequently, the peak flux density in the teeth.

The specific Joule loss (4) is inversely proportional to the tooth length (non normalized), independently of the airgap and the pole pitch.

C. Power factor

With the machine phase currents in time quadrature with the PM flux linkage and neglecting the stator resistance voltage drop, the PF angle φ is expressed in normalized terms as:

$$tan\varphi \cong \frac{4\mu_0}{3\pi} \cdot L_{pole,pu} \cdot \frac{A}{B} \qquad (5)$$

Where $L_{pole,pu}$ is the per-unit phase inductance of the elementary block, whose normalization coefficient is:

$$L_{base} = \frac{\mu_0 \cdot l}{2} \cdot \left(\frac{2}{\pi} \cdot N \cdot k_w\right)^2 \qquad (6)$$

With l being the machine stack length. From (3) and (5) follows that B and A both contribute to produce the shear stress, whilst they are in competition when dealing with the power factor angle: given A and B and then the shear stress, ***the machine PF can be higher or lower according to the per-unit inductance $L_{pole,pu}$***.

In other words, the relationship between the shear stress (read torque) and the power factor depends on the pole per-unit inductance, and wrong design choices can produce machines with a poor power factor, given the torque specification. In the following the minimization of the pole per-unit inductance is addressed, and the criteria for a best compromise between shear stress and power factor are pointed out.

III. MINIMIZATION OF THE POLE INDUCTANCE

The inductance of the elementary block of Fig. 1 (7) is the sum of the *slot* leakage term and the *magnetization* one.

$$L_{pole,pu} = L_{m,pu} + L_{slot,pu} \qquad (7)$$

In normalized quantities, the two terms of (7) depend on the four basic parameters defined in Fig. 1, with expressions that can be different in the cases of distributed, intended as integer q values, and concentrated windings, intended as fractional q values.

A. Distributed winding machines

With integral q, the per-unit magnetization inductance is:

$$L_{m,pu} = \frac{\pi^2}{6 \cdot k_w^2} \cdot \left[1 - \frac{(q-1)^2}{q^3}\right] \cdot \left(\frac{1}{k_c + \frac{l_m}{g}}\right) \cdot \frac{a}{g} \qquad (8)$$

The slot inductance expression is independent of q and it is then valid both for integral and fractional slot numbers:

$$L_{slot,pu} = \frac{\pi^2}{2k_w^2} \cdot \frac{\left(1+\frac{l_m}{g}\right)\cdot\frac{l_t}{g}}{\left[1+\left(1-\frac{k_b B_r}{B_{fe}}\cdot k_t\right)\cdot\frac{l_m}{g}\right]} \cdot \left(\frac{a}{g}\right)^{-1} \quad (9)$$

From (8) and (9) it turns out that L_m is proportional to the ratio a/g, while L_{slot} is inversely proportional to the same quantity.

Fig. 2 shows that an a/g value exists, that minimizes the total per-unit inductance, sum of (8) and (9): it can be demonstrated that the minimum inductance condition corresponds to $L_m = L_{slot}$.

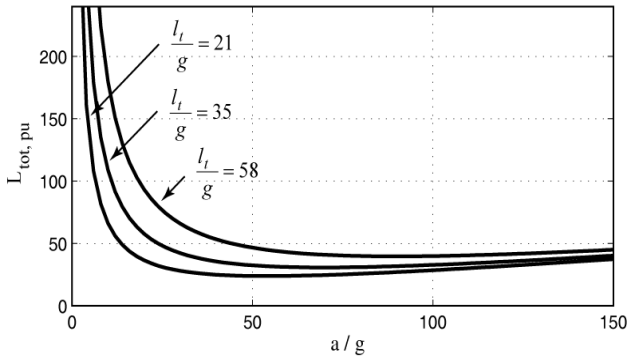

Figure 2. Per-unit pole inductance (8) + (9) for a distributed winding machine having $q = 2$, as a function of a/g, with $l_m/g = 6$ and different l_t/g values.

Posing $L_m = L_{slot}$, the per-unit pole pitch giving the minimum inductance is found, from (8) and (9):

$$\left(\frac{a}{g}\right)_0 = \frac{\sqrt{3}}{\sqrt{1-\frac{(q-1)^2}{q^3}}} \cdot \frac{\left(1+\frac{l_m}{g}\right)\cdot\sqrt{\frac{l_t}{g}}}{\sqrt{1+\left(1-\frac{k_b\cdot B_r}{B_{fe}}\cdot k_t\right)\cdot\frac{l_m}{g}}} \quad (10)$$

The minimum inductance value, corresponding to (10), is:

$$\left(L_{tot,pu}\right)_{min} = \sqrt{1-\frac{(q-1)^2}{q^3}} \sqrt{\frac{\frac{l_t}{g}}{1+\left(1-\frac{k_b B_r}{B_{fe}}k_t\right)\frac{l_m}{g}}} \quad (11)$$

With distributed windings, the effect of q in the formulae (8)-(11) is very limited and the key parameters for pole pitch selection according to (10) turn out to be l_m/g and l_t/g. Typical values of k_t are 0.8 to 0.9 in this case. The choice of l_m/g has been addressed in section II.A. The choice of the tooth length factor l_t/g is more open: as evidenced in Fig. 2, longer teeth increase the pole inductance and would result in a lower power factor, according to (5). However, shorter teeth would increase the specific Joule loss (4), due to the reduction of the copper cross section. A tradeoff between loss and power factor must be found.

B. Single-layer, concentrated winding machines

The slot inductance expression is still (9). $L_{m,pu}$ is now:

$$L_{m,pu} = \frac{\pi^2}{12(qk_w)^2} \cdot \left(\frac{1}{k_c+\frac{l_m}{g}}\right) \cdot \frac{a}{g} \quad (12)$$

In Fig. 3 the per-unit inductance of one pole is reported as a function of a/g for the fractional slot example case $q = 2/7$.

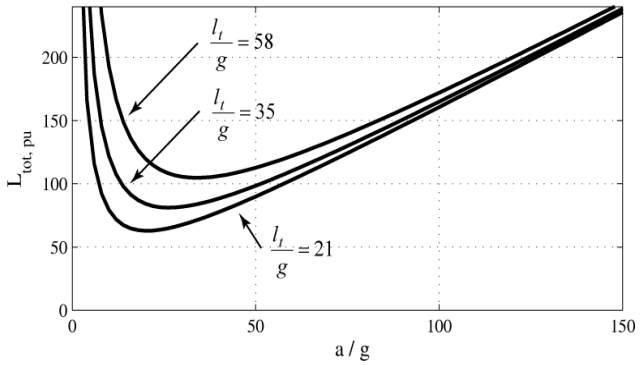

Figure 3. Per-unit pole inductance (10) + (8) for a concentrated winding machine having $q = 2/7$, as a function of a/g, with $l_m/g = 6$ and l_t/g as a parameter.

Posing (9) equal to (12), the minimum inductance condition and the minimum inductance value are now:

$$\left(\frac{a}{g}\right)_0 = \sqrt{6}\cdot q \cdot \frac{\left(1+\frac{l_m}{g}\right)\cdot\sqrt{\frac{l_t}{g}}}{\sqrt{1+\left(1-\frac{k_b\cdot B_r}{B_{fe}}\right)\cdot\frac{l_m}{g}}} \quad (13)$$

$$\left(L_{tot,pu}\right)_{min} = \frac{\pi^2}{\sqrt{6}qk_w^2} \sqrt{\frac{\frac{l_t}{g}}{1+\left(1-\frac{k_b B_r}{B_{fe}}k_t\right)\frac{l_m}{g}}} \quad (14)$$

The pole pitch of minimum inductance (13) is proportional to q this time, while q has little effect in (10), as said.

IV. COMPARISON OF FRACTIONAL AND INTEGRAL SLOT MACHINES

In Figs. 4-6 integer and fractional q numbers are compared in terms of per-unit inductances. Figure 4 reports the pole per-unit inductance as a function of normalized

pole pitch a/g.

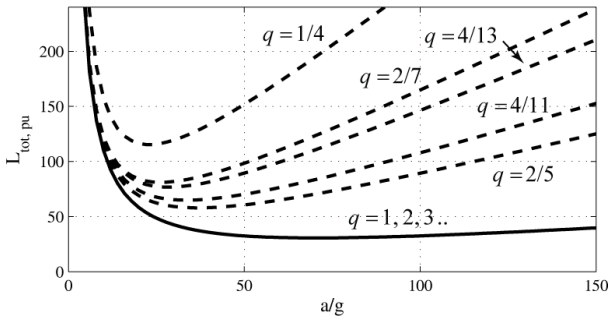

Figure 4. Comparison of the per-unit pole inductance of concentrated (dashed line) and distributed (continuous line) winding machines, all having $l_m/g = 6$ and $l_t/g = 35$.

It turns out that:

- All the curves tend to coincide in the lowest a/g area, where the pole inductance is dominated by the slot term.
- For higher a/g values, fractional slot machines have much higher inductance values, as expected.
- All the curves with integer q are superimposed, while the ones with fractional q can be significantly different, as commented.
- Fractional slot machines have the minimum inductance for lower a/g values than integral slot ones (i.e. at higher pole numbers, in case of rotating machines).

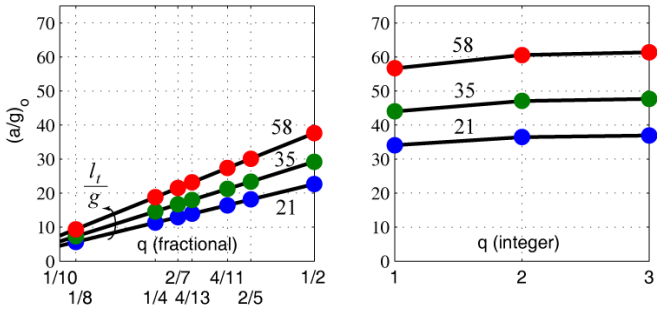

Figure 5. Pole pitch giving the minimum inductance condition (9) or (12), for integer and fractional q, respectively, reported as a function of the slot per pole per phase number and the tooth length. $l_m/g = 6$.

In Figs. 5 the pole pitch of minimum inductance is reported as a function of q values, either fractional (13) or integral (10). In Fig. 6 the corresponding, minimum inductance values are reported, calculated using (11) and (14). In both the figures three different tooth length values l_t/g are considered. From Figs. 5 and 6 turns out that:

- in fractional slot machines, the pole pitch value giving the minimum inductance grows proportionally with the parameter q, as also evident from (13).
- accordingly, the minimum inductance is in inverse proportion with q, when this is fractional (14).
- As a consequence, the difference in inductance between the ones with lower numbers, such as 1/4 or 2/7, and higher numbers, such as 2/5 or 1/2, can be significant.
- The inductance of integral q machines is independent from q and lower than the one of any possible fractional q machine.

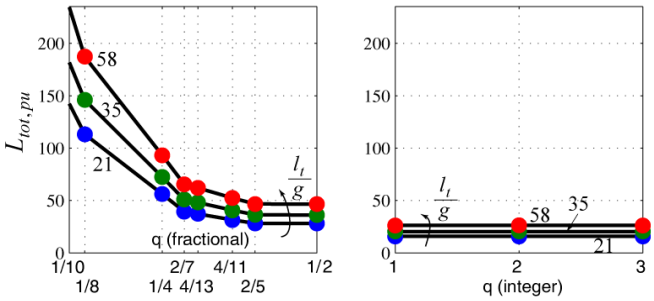

Figure 6. Minimum value of the pole per-unit inductance, corresponding to the pole pitch values of Fig. 5, as a function of the slot per pole per phase number and the tooth length. $l_m/g = 6$.

V. ANALYSIS OF MINIMUM INDUCTANCE MACHINES

For summarizing the analysis presented up to here, the power factor is evaluated at a given shear stress value, for all q values. In Fig. 7 the power factor is reported, according to (5), as a function of q and lt/g, calculated as follows.

The magnetic loading is very similar for all machines, all having $l_m/g = 6$, $B_r = 1.12$ T, $k_b = 1.2$ (e.g. valid for arc magnets with span equal to 5/6). The Carter coefficient is 1.05 for integral q and 1.085 for fractional q. The reference shear stress value is set to 62.5 kN/m^2, and the electric loading is evaluated according to (3). The electric loading is around 55 kA/m in this case. The minimum per-unit inductance is evaluated via (11) and (14). Last, the power factor is calculated via (5) for all machines.

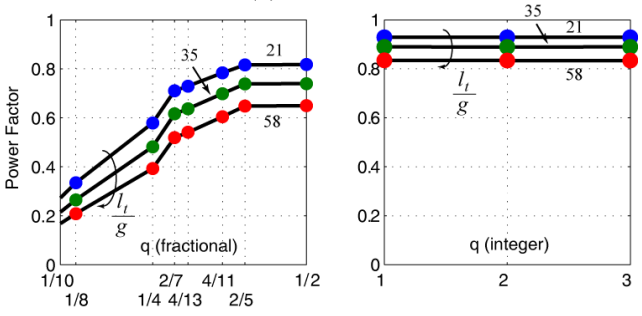

Figure 7. Power factor at same shear stress ($\sigma = 62.5$ kN/m^2) as a function of the slot per pole per phase number and the tooth length. $l_m/g = 6$.

It must be remarked that the machines represented in Fig. 7 have different pole-pitches, calculated according to (10) and (13), that means they would all have different pole numbers, in case of they are rotating machines.

The results of Fig. 7 show that:

- The choice of q is critical for avoiding unacceptable PF values, that is the case with many of the q – l_t/g

combinations of Fig. 7.

- Machines with shorter teeth have a better power factor, but they also have higher specific loss (4).
- Although all the machines are heavily loaded (55 kA/m), the power factor of distributed winding ones is still very high. This can be even too high, for practical applications, determining dangerously high values of short-circuit current. For this reason, integral q machines do not require the strict respect of the minimum per-unit inductance in their design, unless otherwise specified.

It must be remarked that machines with same q and different l_t/g also have a different per unit pitch $(a/g)_0$, in Fig. 7. The plot of the loss factor (4), corresponding to the machines of Fig. 7 is not reported here because it would have required restrictive assumptions about k_{end} and the absolute value of the teeth length. Examples in absolute numbers are given in the following section.

VI. Design flowchart

In this section, the design flowchart is described, based on the per-unit model of the SPM machine. The target is to design a rotating machine. It is then convenient to introduce the relationships between torque and shear stress (15), depending on the rotor radius r and the stack length l, and the expression of the number of poles (16), given the radius and the pole pitch.

$$T = \sigma \cdot 2\pi \cdot \mathrm{r}^2 \cdot \mathrm{l} \qquad (15)$$

$$p = \frac{\pi \cdot \mathrm{r}}{a} \qquad (16)$$

It is assumed that designs with a power factor lower than 0.7 at rated torque should be rejected. In linearity, machines with a power factor lower than 0.7 would have the armature flux linkage higher than the PM flux linkage and, in other words, a disadvantageous oversizing of the power converter given the machine active power.

The flow chart is organized as follows: first, the per-unit model is iteratively utilized for determining the size and performance of the elementary block (subsections *A* and *B*). Then the size and performance of the rotating machine is determined, being this machine the assembly of the just defined elementary block (subsection D).

A. Preliminary data

- Airgap length g
- Type of cooling (upper limit of the specific loss: k_{j0})
- PM grade (B_r) and per-unit thickness l_m/g
- Steel peak exploitation B_{fe}
- Type of winding q

B. Design of the elementary block

1. The magnetic loading B is calculated (1).
2. An expected shear stress value is set, referring to the values that are typical for machines having the same type of cooling
3. The electric loading is calculated from B and σ, according to (3).
4. A tentative tooth length is set and the specific loss is calculated (4), to be compared to upper limit of the specific loss, k_{j0}. Also the end connection factor is a tentative value, to be double checked once the active length of the machine is determined.
5. If k_j is less than or equal to the accepted specific loss then proceed, otherwise step back to point 4, with an augmented tooth length l_t.
6. The pole pitch is determined according to the minimum inductance condition, (10) or (13), respectively.
7. The power factor is evaluated.
8. If PF > 0.7 ok, otherwise l_t is reduced and step back to point 3.

The outputs of this stage are:

- The pole pitch a/g
- The tooth length l_t/g
- The shear stress, the electric loading and the power factor

C. Target machine specification

The final rotating machine is defined according to:

- Target torque T_0 and rated speed.
- Maximum outer diameter, maximum stack length.

D. Design of the rotating machine

Given the calculated shear stress:

9. From (15), the product r^2l is evaluated according to the target torque and the calculated shear-stress.
10. Given r^2l, the rotor radius and stack length are chosen, within the maximum length limit.
11. Once r is chosen, the number of pole pairs (16) is evaluated and truncated to the closest feasible number.
12. The end connection length is evaluated and the specific loss is recalculated according to.
13. Also the machine inductance and the power factor are recalculated, after the pole pitch truncation at step 11.
14. The stator outer radius is calculated
15. If the stator radius exceeds the outer dimension limits, step back to point 10 with a reduced r and an augmented l, whenever possible.
16. If all ok, the design is FEA evaluated

VII. Example designs

Two example machines are designed, one having distributed windings and one with concentrated windings. The target performance is a ***direct-drive wind power generator***, rated 3 MW at 16.9 rpm, that means 1695 kNm

continuous torque. The target heat flow ratio is $k_j \leq 8000$ W/m^2, referring to direct wind ventilation. The stator diameter must be lower than or equal to 4 m.

At first, the flowchart of section VI is applied to the design of the concentrated windings machine, indicated as ***design 1***. The number of slot per pole per phase is $q = 2/5$, that showed to give better power factor values than most of the other fractional values according to the presented analysis (e.g. Fig. 7). The design procedure is iterated for obtaining a stator radius that is exactly 2 m and to comply with the power factor and loss constraints. The geometry of the resulting design is summarized in the left column of Table I, along with the main input and coefficients to be used in the formulae. In Fig. 8 (top) the sketch of the laminations is also reported. The model calculated performance, is reported in Table II. The minimum inductance condition (13) has been pursued, as described in the design flowchart, and the calculated PF is 0.7, at the bottom of the accepted range.

TABLE I – GEOMETRY OF THE TWO EXAMPLE DESIGNS

		Design 1 concentrated windings	***Design 2*** distributed windings
Slot/pole/phase	q	2/5	1
Magnet grade	Br	1.12 T	
Airgap	g	5 mm	
Core flux density	B_{fe}	1.5 T	
PM length	l_m/g	6.1	
Stator radius	R	2 m	2 m
Rotor radius	r	1.840 m	1.782 m
Stack length	l	1.3 m	1.3 m
Pole pitch	a/g	19.3	25.0 **
Tooth length	l_t/g	23.7 *	35.27 ***
Pole pairs	p	60	45
Yoke length	l_y	23.6 mm	30.5 mm
Carter	k_c	1.085	1.05
End connections	k_{end}	1.093	1.41
Tooth scaling	k_t	0.73	0.8
Slot filling	k_{Cu}	0.4	0.4

** Designed for PF = 0.707, according to (5)*
*** Lower than (10), giving the minimum inductance*
**** Chosen for having the same k_j (4) of the design 1*

The distributed winding example, called ***design 2***, has $q = 1$, for having the slots not too slender that would cause the winding to be hardly feasible. The geometry of *design 2* is described in Table I and the calculated performance in Table III. The sketch of the laminations is in Fig. 8 (bottom).

The design flowchart applied in this case has some differences with respect to section VI: instead of the minimum inductance condition (10), that would have led to $(a/g)_0 = 44.19$, a lower pole pitch factor $a/g = 24.95$ has been selected, corresponding to a higher pole number with shorter end connections and still giving a good power factor (0.80 in Table III). Moreover, the tooth length has been chosen for ***having the same specific loss of design 1***, according to (4), for making the comparison of the two machines more straightforward. According to the design target, the output machine has the same stator outer diameter, the same calculated torque and Joule loss of *design 1*, with longer teeth and then a smaller rotor diameter. This means the shear stress is no longer a uniform metric for the comparison of the two example designs: the model and FEA calculated torque will be used instead in the following. Iron loss is not included in the comparison, due to the low fundamental frequency of the example application.

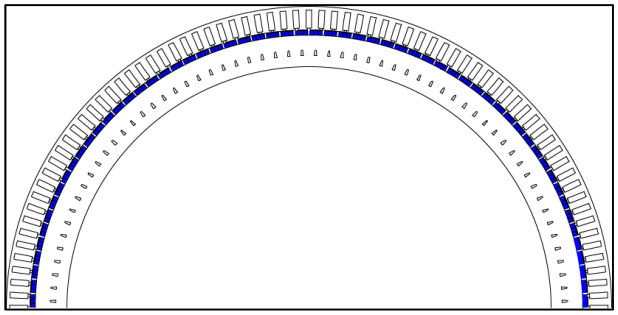

(*design 1* - $q = 2/5$)

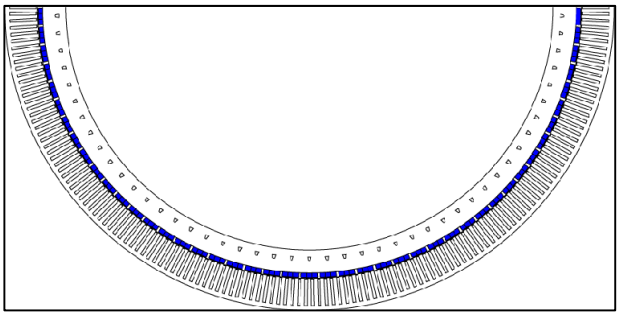

(*design 2* - $q = 1$)

Figure 8. Sketches of the laminations of the two example deisgns.

A. Finite element validation of the model

The per-unit design procedure is validated via static magnetic FEA runs in FEMM [9]. Finite element results are given in Tables II and III, aside the model results for the two example designs.

TABLE II – PERFORMANCE OF DESIGN 1, q = 2/5

	Eq.	Model	FEA
B	(1)	1.14 T	1.09 T
A	(2)	53496 A/m	
σ		60.99 kN/m^2	52.99 kN/m^2
k_j	(4)	6821 W/m^2	6275 W/m^2
T	(15)	1695 kNm	1473 kNm
Phase current		4278 Apk	
Phase voltage		664 Vpk	577 Vpk
Joule loss		111.4 kW	102.5 kW
L_m	(12)	8.78 mH	
L_{slot}	(9)	8.83 mH 15.38 mH*	
L_{tot}		17.61 mH 24.16 mH*	25.76 mH
PF		0.7*	0.7

** Tooth tip inductance included*

TABLE III – PERFORMANCE OF DESIGN 2, q = 1

	Eq.	Model	FEA
B	(1)	1.145T	1.11 T
A	(2)	56748	
σ	(3)	64.99 kN/m^2	57.78 kN/m^2
k_j	(4)	6821 W/m^2	6017 W/m^2
T	(15)	1695 kNm	1507 kNm
Phase current		3715 A pk	
Phase voltage		671 V pk	577 V pk
Joule loss		111.4 kW	98.3 kW
L_m	(8)	2.55 mH	
L_{slot}	(9)	8.1 mH 9.7 mH*	
L_{tot}		10. 65 mH 12.25 mH*	11.87 mH
PF		0.80*	0.83

** Tooth tip inductance included*

The magnetic loading is FEA evaluated at no load, and the model is very accurate in this case. The electric loading is set to be equal purposely, as also the Joule loss (specific and total) should be. The number of turns in series per phase has been chosen to have a phase voltage of 577 V peak at rated current, for both machines.

The discrepancy between FEA and model evaluated losses in Table II and III is related to the effect of curvature, more evident in *design 2*: in fact, the adopted linear model underestimates the cross section of slots, and the error is more evident with longer teeth. Anyway, the model approximation is conservative in this case.

An important difference between the model and FEA is the tooth tip inductance term, that is not included in the expression used for slot inductance evaluation (9). The tooth tip term can be calculated accurately, and in fact it is added to the model calculated inductance values of Tables II and III, giving out the "starred" inductance value of the two tables. The tooth tip inductance is not included in (9) because this would have required the definition of a lot of additional parameters, since the tooth tip per-unit shape can vary a lot from case to case.However, the minimum inductance pole pitch condition (10) and (13) is not affected by the neglected inductance term, whose only effect is to increase the total inductance according to the tooth tip shape and then lower the power factor slightly with respect to the calculated one.

B. Effect of core saturation

The main difference between FEA and the model is the underestimate of the shear stress and then the torque. This difference is generated by core saturation, not accounted for in the model. As said in the first part of the paper, the design parameter B_{fe} is the one that determines the yoke and tooth dimensions, referring to the willed core exploitation, evaluated at no load. B_{fe} set to 1.5 T in the example designs. This means that when the machine is loaded the stator core will actually work at higher values of local flux density, due to the armature flux, in particular for those machines having a high armature flux indicated by a low power factor.

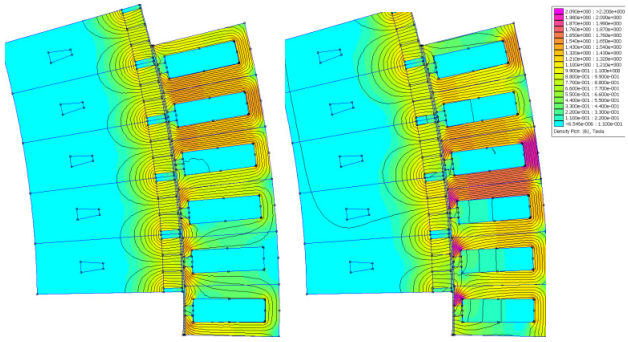

(no load) (I_q = 4278 A pk)

Figure 9. Field density disctribution of design2 at no load and rated load Flux density scale between 0 and 2.09 T.

In Figs. 9 and 10 the flux density maps of the two designs are reported, showing both no load and rated load conditions. In *design 1*, the peak flux density at no load is 1.5 T (yoke and tooth) and 2.05 T (yoke) and 1.70 T (tooth) at load. *Design 2*: 1.55 T at no load (yoke and tooth); 1.65 (yoke) and 1.75(tooth) at load.

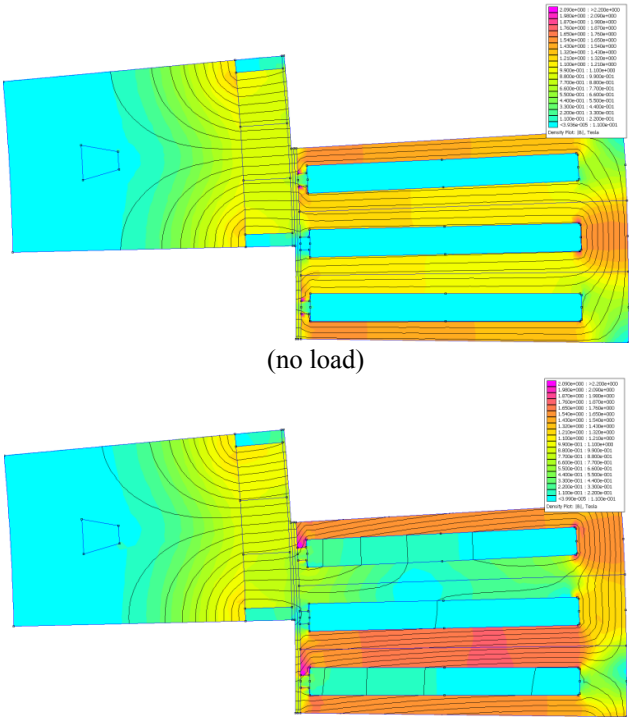

Figure 10. Field density disctribution of design1 at no load and rated load. Flux density scale between 0 and 2.09 T.

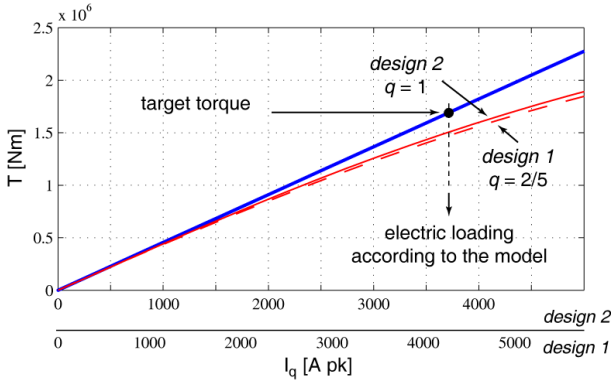

Figure 11. Machine torque according to the linear model and the FEA, as a function of the machine current, for the two designs, to put in evidence the effect of core aturation.

Torque saturation as a function of electric loading is FEA evaluated and reported in Fig. 10, for the two machines, for putting in evidence once more the accuracy of the model in linearity, and to quantify the effect of having disregarded saturation. Torque saturation is somehow expected by machine designers and it is limited although significant in both designs, at the calculated electric loading. The plots in Fig. 11 have different Ampere scales due to the different numbers of turns of the two machines. One possible countermeasure against the torque overestimate due to saturation, with no modification of the proposed design approach, is to choose a lower B_{fe} (e.g. 1.4 T), in particular when the machine inductance is such as the armature flux is not negligible. Also the model estimated voltage is higher than the FEA calculated one, both in Table II and Table III, still due to core saturation.

VIII. Conclusion

The design of surface mounted permanent magnet motors with high number of poles is approached by means of a per unit linear model. Design examples are provided and FEA validated for the case of a large size, direct drive wind generator. The concentrate winding design, as expected, has a lower power factor, and the choice of the slot/pole combination might have a very negative impact on this aspect. A low power factor also means a large armature flux at load, and then torque saturation due to core saturation. The distributed winding design has longer teeth, for having the same Joule loss, due to the longer end connections. Core saturation at load is lower but still evident also in this case. Iron loss are not significant for the chosen application but could enter the game in case of higher speed ratings. Single layer concentrated windings are considered, only: double layer versions could give, in general, a better performance.

References

[1] Jahns, T.M.; "The expanding role of PM machines in direct-drive applications," Electrical Machines and Systems (ICEMS), 2011 International Conference on , vol., no., pp.1-6, 20-23 Aug. 2011

[2] EL-Refaie, A.M.; , "Fractional-Slot Concentrated-Windings Synchronous Permanent Magnet Machines: Opportunities and Challenges," Industrial Electronics, IEEE Transactions on , vol.57, no.1, pp.107-121, Jan. 2010

[3] Mecrow, B.C.; Jack, A.G.; Haylock, J.A.; Coles, J.; , "Fault-tolerant permanent magnet machine drives," Electric Power Applications, IEE Proceedings - , vol.143, no.6, pp.437-442, Nov 1996

[4] Magnussen, F.; Sadarangani, C.; , "Winding factors and Joule losses of permanent magnet machines with concentrated windings," *Electric Machines and Drives Conference, 2003. IEMDC'03. IEEE International* , vol.1, no., pp. 333- 339 vol.1, 1-4 June 2003

[5] Bianchi, N.; Bolognani, S.; Frare, P.; , "Design criteria for high-efficiency SPM synchronous motors," *Energy Conversion, IEEE Transactions on* , vol.21, no.2, pp. 396- 404, June 2006

[6] El-Refaie, A.M.; Jahns, T.M.; Novotny, D.W.; , "Analysis of surface permanent magnet machines with fractional-slot concentrated windings," *Energy Conversion, IEEE Transactions on* , vol.21, no.1, pp. 34- 43, March 2006

[7] El-Refaie, A.M.; Zhu, Z.Q.; Jahns, T.M.; Howe, D.; , "Winding Inductances of Fractional Slot Surface-Mounted Permanent Magnet Brushless Machines," *Industry Applications Society Annual Meeting, 2008. IAS '08. IEEE* , vol., no., pp.1-8, 5-9 Oct. 2008

[8] Soong, W.L.; Miller, T.J.E.; , "Field-weakening performance of brushless synchronous AC motor drives," Electric Power Applications, IEE Proceedings - , vol.141, no.6, pp.331-340, Nov 1994

[9] D. C. Meeker, Finite Element Method Magnetics, Version 4.0.1 (03Dec2006 Build), http://www.femm.info